

# GENERALISED QPLEXES, SIMILARITY TO QUANTUM STATE SPACE, AND 2-DESIGNS

ANNA SZYMUSIAK AND WOJCIECH SŁOMCZYŃSKI

**ABSTRACT.** We study the class of quantum measurements with the property that the image of the set of quantum states under the measurement map transforming states into probability distributions is similar to this set. This leads to the generalisation of the notion of a qplex, where SIC-POVMs are replaced by the elements of the much larger class of 2-design POVMs. The intrinsic geometry of a generalised qplex is the same as that of the set of quantum states, so we explore its external geometry, investigating, inter alia, the algebraic and geometric form of the inner (basic) and the outer (primal) polytopes between which the generalised qplex is sandwiched. In particular, we examine generalised qplexes generated by MUB-like 2-design POVMs utilizing their graph-theoretical properties. Our paper is the first step towards an abstract definition of a generalised qplex.

## 1. INTRODUCTION

Over the last ten years in a series of papers [2, 3, 30–33, 48, 67] Fuchs, Schack, Appleby, Stacey, Zhu and others have introduced first the idea of *QBism* (*quantum Bayesianism*) and then its probabilistic embodiment - the (*Hilbert*) *qplex*, both based on the notion of *symmetric informationally complete positive operator valued measure* (*SIC-POVM*) representing the standard (or reference) measurement of a quantum system. In spite of the fact that SIC-POVMs do indeed exhibit some unique properties that distinguish them among other IC-POVMs [24–26, 51], we believe that similar (or, in a sense, even richer from purely mathematical point of view) structures, say, *generalised qplexes*, can be successfully used to faithfully represent quantum states as probability distributions if we replace SIC-POVMs with the broader class of rank-1 measurements generated by *complex projective 2-designs*<sup>1</sup>.

In standard (finite)  $d$ -dimensional quantum mechanics the states of a system are identified with the set of positive trace-one operators  $\mathcal{S}(\mathbb{C}^d)$  (known also as density operators or density matrices) and the pure states with the extreme boundary of this set,  $\mathcal{P}(\mathbb{C}^d)$ , i.e. the rank-1 orthogonal projections or, equivalently, with the elements of the projective complex vector space  $\mathbb{C}\mathbb{P}^{d-1}$ . The quantum states can be also described as the elements of the  $(d^2 - 1)$ -dimensional real Hilbert space  $\mathcal{L}_s^0(\mathbb{C}^d)$  of Hermitian traceless operators on  $\mathbb{C}^d$ , endowed with the Hilbert-Schmidt product given by  $(\sigma|\tau) := \text{tr}(\sigma\tau)$  for  $\sigma, \tau \in \mathcal{L}_s^0(\mathbb{C}^d)$ . Namely, the map  $\mathcal{S}(\mathcal{H}) \ni \rho \rightarrow \rho - I/d \in \mathcal{L}_s^0(\mathbb{C}^d)$  gives us an affine embedding of the set of states (resp. pure states) into the (*outer*)  $(d^2 - 1)$ -dimensional ball (resp. sphere) in  $\mathcal{L}_s^0(\mathbb{C}^d)$  centred at 0 of radius  $\sqrt{1 - d^{-1}}$ . The image of this map is called the *Bloch body* (resp. the *generalised Bloch sphere*). Only for  $d = 2$  the map is onto, and for  $d > 2$  its image is a convex subset of the ball of full dimension and contains the maximal (*inner*) ball of radius  $1/\sqrt{d(d-1)}$  [6].

A measurement with a finite number  $n$  of possible outcomes can be described by a *positive operator valued measure* (*POVM*), i.e. an ensemble of positive non-zero operators  $\Pi = (\Pi_j)_{j=1, \dots, n}$  on  $\mathbb{C}^d$  that sum to the identity operator, i.e.  $\sum_{j=1}^n \Pi_j = I$ . According to the *Born rule*, the affine *measurement map*  $p_\Pi$  sends an input quantum state  $\rho \in \mathcal{S}(\mathbb{C}^d)$  into the vector of probabilities of the respective outcomes  $(\text{tr}(\rho\Pi_j))_{j=1, \dots, n}$  that belongs to the *standard (probability) simplex*  $\Delta_n$ . If this map is one-to-one, we call  $\Pi$  *informationally complete*; then, necessarily,  $n \geq d^2$ . In this situation the results of the measurement uniquely determine the input state, and so *quantum tomography*, i.e. the task of reconstructing the quantum state from the outcomes of the measurement, can be concluded. In this case  $\mathcal{Q}_\Pi := p_\Pi(\mathcal{S}(\mathbb{C}^d))$  (the *probability range* of  $\Pi$ ) is an affine  $(d^2 - 1)$ -dimensional image of  $\mathcal{S}(\mathbb{C}^d)$  and so, clearly,  $\text{ext}\mathcal{Q}_\Pi = p_\Pi(\mathcal{P}(\mathbb{C}^d))$ . We shall analyse the structure of the image of  $p_\Pi$  in Sections 2 and 3. The main result of the present paper, Theorem 3, provides a necessary and sufficient condition for  $\mathcal{S}(\mathbb{C}^d)$  and  $\mathcal{Q}_\Pi$  to be of the same shape (similar): the orthogonal projections onto  $\mathcal{L}_s^0(\mathbb{C}^d)$  of the effects constituting the POVM in question need to form a tight operator frame in this space. In consequence, we can identify the set of quantum states with a convex subset of  $\Delta_n$ .

<sup>1</sup>In fact, Fuchs and Schack considered such an idea in [30], but it seems that they rejected it. See also [75].

In this paper we pay special attention to POVMs such that  $\Pi_j$  ( $j = 1, \dots, n$ ) are one-dimensional and of equal trace, and so proportional to certain pure states  $\rho_j$  ( $j = 1, \dots, n$ ). We show that in this case  $p_\Pi$  is a similarity if and only if these states constitute a complex projective 2-design (Corollary 5), or, equivalently, their image in the Bloch body under natural embedding is a tight frame in  $\mathcal{L}_s^0(\mathbb{C}^d)$ . Then we call  $\mathcal{Q}_\Pi$  a *generalised (Hilbert) qplex*. Note that the class of 2-designs also contains, besides SIC-POVMs [34], also complete sets of MUBs (mutually unbiased bases) [49], MUB-like designs [46], orbits of the multiqubit Clifford group [84] (in fact, the latter are 3-designs), group designs [38], and many other discrete objects representing quantum measurements [6, 7, 9].

The main difference between (Hilbert) qplexes and their generalisation lies not in their intrinsic geometry, but rather in their external geometry (i.e. the location in the underlying real vector space) we describe in detail in Section 7. Both a (Hilbert) qplex and a (Hilbert) generalised qplex are isomorphic (similar) through the measurement map to the space of quantum states (or, to put it another way, the Bloch body). The former, however, is a subset of the standard  $(d^2 - 1)$ -dimensional simplex  $\Delta_{d^2}$  lying in a  $d^2$ -dimensional real vector space, whilst the latter is a subset of a  $(d^2 - 1)$ -dimensional *primal polytope*  $\Delta$  which is a *cross-section* of the ‘larger’ simplex  $\Delta_n$ . We show that the cross-section in question has to be *central*, i.e. it passes through the centre of the simplex  $c_n$ , and, what is more, *medial*, i.e. the vertices of the simplex are equidistant from the *primal affine space*  $\mathcal{A}$  generated by  $\Delta$ . (We borrow the term ‘medial’ from [77, 82], though the authors considered only hyperplane sections there.) It seems that the latter property is crucial for constructing a generalised qplex. The distance equal to  $1 - d^2/n$  measures the deviation from minimality: for  $n = d^2$  we get necessarily a SIC-POVM. Moreover, we consider another polytope, namely a *basis polytope*  $D$  generated by the elements of a 2-design transformed by  $p_\Pi$ . This polytope is the image under the homothety (with centre at  $c_n$  and ratio  $1/(d+1)$ ) of the orthogonal projection of  $\Delta_n$  on  $\mathcal{A}$ .

The generalised qplex  $\mathcal{Q}_\Pi$  is a convex set sandwiched between these two polytopes  $D$  and  $\Delta$ . The situation is somewhat analogous to the quantum (Bell) correlation picture, where the quantum convex body lies in-between the *local polytope* [63] and the *non-signalling polytope* [65], see also [13, 14, 29, 35, 36, 66], or to the related idea of applying graph theoretical concepts [39, 50] to the analysis of quantum contextuality, where the probabilities of the results of an experiment in classical, quantum, and more general probabilistic theories are described by, respectively, *stable set polytope*  $\subset$  *theta body*  $\subset$  *fractional stable set polytope* (or, in other words, *clique-constrained stable set polytope*) of the graph related to the experiment [1, 16, 17]. In fact, the analogy is even deeper since also in our situation  $D$  and  $\Delta$  represent, in a sense, classical and ‘beyond-quantum’ behaviour, respectively.

The polytopes  $D$  and  $\Delta$  are *dual* in  $\mathcal{A}$ , see [80], namely  $D$  and  $\iota(\Delta)$ , where  $\iota$  is the inversion through  $c_n$ , are *polar* with respect to the central sphere of radius  $m := n^{-1/2}(d+1)^{-1/2}$ . Moreover,  $\mathcal{Q}_\Pi$  is *self-dual* in this sense, every pair of elements  $p, q \in \mathcal{Q}_\Pi$  fulfils the fundamental inequalities:  $dm^2 \leq \langle p, q \rangle \leq 2dm^2$ , and  $\mathcal{Q}_\Pi$  lies in-between two central balls: the inscribed ball of  $\Delta$  of radius  $r := m(d-1)^{-1/2}$  and the circumscribed ball of  $D$  of radius  $R := m(d-1)^{1/2}$ . Note that  $m = \sqrt{rR}$ . Thus, the overall geometric picture is similar to the (Hilbert) qplex case represented schematically in [2, Fig. 2 and 3], but more complicated as our polytopes are not necessarily simplices. These properties, especially the mediality of the constitutive cross-section space  $\mathcal{A}$ , can be chosen as a starting point for an abstract definition of generalised qplex (in preparation).

This geometric approach can be supplemented by an algebraic one we present in Section 4, namely, for the extreme boundary  $\text{ext}\mathcal{Q}_\Pi$  of the qplex we show that it can be described by a set of polynomial equations (Theorem 6):  $n$  linear, one quadratic, and one cubic (for  $d > 2$ ). The system of  $n$  linear equations defining the affine space  $\mathcal{A}$  is just an analogue of the famous primal equation (‘Urgleichung’) known from the QBism theory where  $\Pi$  plays the role both of ‘ground’ and ‘sky’ measurement. Note, however, that for SIC-POVMs these equations do not impose any constraints on probabilities as they are always satisfied (Corollary 7.(ii)). For low-dimensional systems ( $d = 2, 3$ ) we provide also the description of the whole generalised qplex  $\mathcal{Q}_\Pi$  with the help of a set of polynomial equations and inequalities (Corollary 8).

We complete our paper with a detailed analysis of several examples of 2-designs and the corresponding generalised qplexes: cubical, cuboctahedral and icosahedral POVMs in dimension 2, as well as SIC-POVMs in dimension 3 in Section 6.3. The linear equations defining primal affine space  $\mathcal{A}$  take an unexpectedly simple form for complete sets of MUBs and MUB-like 2-designs (i.e. two-distance 2-designs with one of distances equal to 0), see Section 6. Apart from complete sets of MUBs, we know four sporadic objects of this type, one in each of dimensions 4, 5, 6 and 28, and they all generate the orthogonality graph on the elements of the POVM that is a strongly regular graph with some special

properties. In this case the equations describing  $\mathcal{A}$  can be replaced by the requirement that *the sum of the probabilities over each orthonormal basis is constant* (Theorem 9).

Finally, we would like to mention that figuring out how the qplex  $\mathcal{Q}_\Pi$  is located inside the simplex  $\Delta_n$  may provide a way to solve the problems of minimising and maximising the Shannon entropy of POVM problem. This in turn leads to the understanding of the lower and upper bounds for the uncertainty of the measurement results [10, 22, 23, 58, 70, 72–74].

## 2. THE PROBABILITY RANGE OF POVMs

Let us consider a quantum system represented by  $\mathbb{C}^d$  and a general discrete quantum measurement on it described by a POVM (positive operator valued measure)  $\Pi = \{\Pi_i\}_{i=1}^n$ . In particular, if  $\Pi_i$  are orthogonal projections, we call  $\Pi$  a PVM (projection valued measure). Let us denote by  $\mathcal{Q}_\Pi$  the set of ‘allowed’ probabilities, i.e. the set of all possible probability distributions of the measurement outcomes over all quantum states. It is known also as the *probability range* of  $\Pi$  [40]. More formally, if we denote by  $\mathcal{L}_s(\mathbb{C}^d)$  the  $d^2$ -dimensional real Hilbert space of Hermitian operators on  $\mathbb{C}^d$  endowed with the Hilbert-Schmidt inner product, then

$$\mathcal{Q}_\Pi := p_\Pi(\mathcal{S}(\mathbb{C}^d)),$$

where

$$p_\Pi : \mathcal{L}_s(\mathbb{C}^d) \ni A \mapsto (\text{tr}(A\Pi_1), \dots, \text{tr}(A\Pi_n)) \in \mathbb{R}^n$$

is a positive linear map. We introduce also  $\mathcal{Q}_\Pi^1$  for the probability distributions attained for the pure states, i.e.

$$\mathcal{Q}_\Pi^1 := p_\Pi(\mathcal{P}(\mathbb{C}^d)).$$

As a straightforward consequence, we get the following properties of  $\mathcal{Q}_\Pi$  and  $\mathcal{Q}_\Pi^1$ :

*Fact 1.*  $\mathcal{Q}_\Pi = \text{conv}(\mathcal{Q}_\Pi^1)$  and  $\text{ext}(\mathcal{Q}_\Pi) \subset \mathcal{Q}_\Pi^1$ .

Let us recall that the *joint numerical range* of Hermitian matrices  $A_1, A_2, \dots, A_n$  is defined by

$$\mathcal{F}(A_1, A_2, \dots, A_n) = \{(\langle z|A_1|z\rangle, \langle z|A_2|z\rangle, \dots, \langle z|A_n|z\rangle)^T | z \in \mathbb{C}^d, \|z\| = 1\} \subset \mathbb{R}^n.$$

As any pure state  $\rho$  is necessarily the orthogonal projection onto some unit vector  $z \in \mathbb{C}^d$ , we have  $\text{tr}(\rho\Pi_j) = \langle z|\Pi_j|z\rangle$ , and so  $\mathcal{Q}_\Pi^1$  can be described also as the joint numerical range of  $\Pi_1, \Pi_2, \dots, \Pi_n$ .

We are particularly interested in the shape of  $\mathcal{Q}_\Pi$ . For  $d = 2$ ,  $\mathcal{Q}_\Pi$  is an ellipsoid, possibly degenerated, as a linear image of 3-dimensional ball. Some examples of these ellipsoids are presented below.

**Example 1.** Let us consider a one-parameter family of rank-1 normalized POVMs on  $\mathbb{C}^2$  consisting of  $n = 4$  effects:

$$\begin{aligned} \Pi_1 &:= \frac{1}{4} \begin{pmatrix} 1 + \sin \alpha & \cos \alpha \\ \cos \alpha & 1 - \sin \alpha \end{pmatrix}, \quad \Pi_2 := \frac{1}{4} \begin{pmatrix} 1 + \sin \alpha & -\cos \alpha \\ -\cos \alpha & 1 - \sin \alpha \end{pmatrix}, \\ \Pi_3 &:= \frac{1}{4} \begin{pmatrix} 1 - \sin \alpha & -i \cos \alpha \\ i \cos \alpha & 1 + \sin \alpha \end{pmatrix}, \quad \Pi_4 := \frac{1}{4} \begin{pmatrix} 1 - \sin \alpha & i \cos \alpha \\ -i \cos \alpha & 1 + \sin \alpha \end{pmatrix}, \end{aligned}$$

where  $\alpha \in [0, \pi/2]$ . The pure states  $\rho_i = 2\Pi_i$  for  $i = 1, \dots, 4$  are represented on the Bloch sphere by the vertices of certain tetragonal disphenoid, i.e. a tetrahedron whose four faces are congruent isosceles triangles. Such a tetrahedron can be uniquely characterized by the length of the base (or legs) of that triangle. Taking into account possible degenerations, we get five cases. For  $\alpha = \frac{\pi}{2}$  the disphenoid degenerates to a segment (length of the base = 0) and the measurement effectively acts as the projective von Neumann measurement. For  $\alpha \in (0, \pi/2)$  there is no degeneracy and the POVM is informationally complete. In particular, for  $\alpha \in (\arcsin \frac{1}{\sqrt{3}}, \frac{\pi}{2})$  the length of the base of the face triangle is less than the length of its legs. For  $\alpha = \arcsin \frac{1}{\sqrt{3}}$  we get the tetrahedron (faces being equilateral triangles) representing SIC-POVM, the only case of 2-design here. For  $\alpha \in (0, \arcsin \frac{1}{\sqrt{3}})$  the disphenoid is such that the length of the base of the face triangle is greater than the length of its legs. Finally, for  $\alpha = 0$  the disphenoid degenerates to a square (length of the legs = 0) representing a non-informationally complete highly symmetric POVM. Its probability range in these cases is presented in Fig. 1 and evolves as follows: for  $\alpha = \frac{\pi}{2}$  we obtain a segment, then for  $\alpha \in (0, \pi/2)$  – an elongated spheroid, for  $\alpha = \arcsin \frac{1}{\sqrt{3}}$  – a sphere, for  $\alpha \in (0, \arcsin \frac{1}{\sqrt{3}})$  – a flattened spheroid and, finally, for  $\alpha = 0$  – a disk.

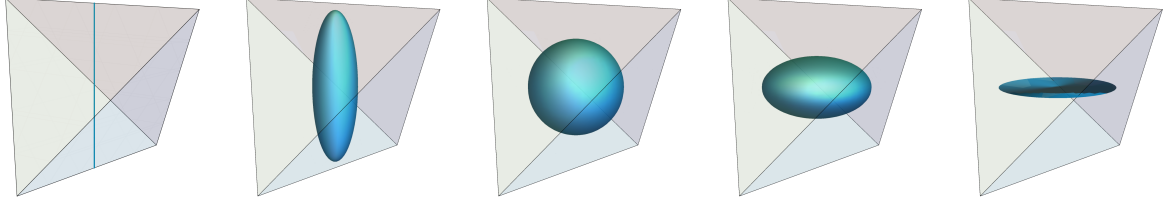


FIGURE 1.  $\mathcal{Q}_\Pi$  in the cases:  $\alpha = \frac{\pi}{2}$  – a segment;  $\alpha \in (0, \pi/2)$  – an elongated spheroid;  $\alpha = \arcsin \frac{1}{\sqrt{3}}$  – a sphere;  $\alpha \in (0, \arcsin \frac{1}{\sqrt{3}})$  – a flattened spheroid;  $\alpha = 0$  – a disk. All solids are tangent to  $\Delta_4$ .

It is much more difficult to describe the shape of  $\mathcal{Q}_\Pi$  in dimensions higher than 2. However, it seems that there are two cases which are in some sense ‘nice’. The first one is when  $\mathcal{Q}_\Pi$  is the full simplex. The second one is when it is of the same shape as  $\mathcal{S}(\mathbb{C}^d)$ . In what follows we deal with the sufficient and necessary conditions for these two to appear. As for the full simplex case, the following characterization may be categorized as quantum information folklore (see, e.g. [40, p. 4]). The second case will be thoroughly analysed in the next section.

**Definition 1.** We say that a POVM  $\Pi$  has the *norm-1-property* if  $\|\Pi_i\| = 1$  for  $i = 1, \dots, n$  (here  $\|A\| = \max_{\|x\|_2=1} \|Ax\|_2$ ).

**Theorem 1.**  $\mathcal{Q}_\Pi = \Delta_n$  if and only if  $\Pi$  has the norm-1-property. Moreover, in such case,  $\mathcal{Q}_\Pi^1 = \Delta_n$ ,  $n \leq d$  and  $n = d$  if and only if  $\Pi$  is a rank-1 PVM.

### 3. THE PROBABILITY RANGE SIMILAR TO QUANTUM STATE SPACE

In order to provide a characterization of the second case we need to make some preparations. From now on for  $A, B \in \mathcal{L}_s(\mathbb{C}^d)$  we will denote their Hilbert-Schmidt inner product by  $(A|B)$  and the induced norm of  $A$  by  $\|A\|_{HS}$ . We also consider  $\mathcal{L}_s^0(\mathbb{C}^d) := \{A \in \mathcal{L}_s(\mathbb{C}^d) | \text{tr}A = 0\}$ , i.e. the  $(d^2 - 1)$ -dimensional subspace of traceless Hermitian operators. It is easy to see that

$$\pi_0 : \mathcal{L}_s(\mathbb{C}^d) \ni A \mapsto A - (\text{tr}A/d)I \in \mathcal{L}_s(\mathbb{C}^d)$$

is the orthogonal projection onto  $\mathcal{L}_s^0(\mathbb{C}^d)$ . The following definition gives a precise description of what we mean by ‘the same shape’ in terms of similarity:

**Definition 2.** We say that  $\mathcal{Q}_\Pi$  is *similar* to quantum state space  $\mathcal{S}(\mathbb{C}^d)$  if there exists  $\alpha > 0$  such that

$$(1) \quad \|p_\Pi(\rho) - p_\Pi(\sigma)\|^2 = \alpha \|\rho - \sigma\|_{HS}^2 \quad \text{for all } \rho, \sigma \in \mathcal{S}(\mathbb{C}^d).$$

*Remark 1.* The above definition can be expressed equivalently as

$$(2) \quad \langle p_\Pi(\rho) - c_\Pi, p_\Pi(\sigma) - c_\Pi \rangle = \alpha \langle \rho - I/d, \sigma - I/d \rangle$$

for all  $\rho, \sigma \in \mathcal{S}(\mathbb{C}^d)$ , where  $c_\Pi := p_\Pi(I/d) = (\text{tr}\Pi_1/d, \dots, \text{tr}\Pi_k/d)$ . (Note that  $\rho - I/d = \pi_0(\rho)$  and  $p_\Pi(\rho) - c_\Pi = p_\Pi(\pi_0(\rho))$ .) In particular,  $p_\Pi|_{\mathcal{L}_s^0(\mathbb{C}^d)}$  is a similarity with similarity ratio  $s = \alpha^{1/2}$ .

Let us recall some basic facts about finite tight frames. Let  $V$  be a finite-dimensional Hilbert space with inner product  $\langle \cdot | \cdot \rangle$  and let  $F := \{f_1, \dots, f_m\} \subset V$ .

**Definition 3.**  $F$  is a *frame* if there exist  $\alpha, \beta > 0$  such that

$$\alpha \|v\|^2 \leq \sum_{i=1}^m |\langle v | f_i \rangle|^2 \leq \beta \|v\|^2 \quad \text{for all } v \in V.$$

$F$  is called a *tight frame* if  $\alpha = \beta$ . In such situation  $\alpha$  is referred to as the *frame bound*. The operator  $S := \sum_{i=1}^m |f_i\rangle\langle f_i|$  is called the *frame operator*.

**Theorem 2.** *The following conditions are equivalent:*

- i.  $F$  is a tight frame with frame constant  $\alpha$ ;
- ii.  $\sum_{i=1}^m \langle u | f_i \rangle \langle f_i | v \rangle = \alpha \langle u | v \rangle$  for all  $u, v \in V$ ;
- iii.  $S = \alpha I$ .

*Proof.* See, e.g. [79]. □

Now we can proceed to the characterization of POVMs for which  $\mathcal{Q}_\Pi$  is similar to the quantum state space.

**Theorem 3.** *Let  $\Pi$  be a POVM. Then  $\mathcal{Q}_\Pi$  is similar to the quantum state space if and only if  $\pi_0(\Pi)$  is a tight (operator) frame in  $\mathcal{L}_s^0(\mathbb{C}^d)$ . Moreover, the frame bound and the square of similarity ratio coincide and are equal to*

$$\alpha = \frac{1}{d^2 - 1} \left( \sum_{i=1}^n \text{tr} \Pi_i^2 - \frac{1}{d} \sum_{i=1}^n (\text{tr} \Pi_i)^2 \right).$$

*Proof.* Since  $\text{span}\{\rho - I/d : \rho \in \mathcal{S}(\mathbb{C}^d)\} = \mathcal{L}_s^0(\mathbb{C}^d)$ , it follows that (2) holds for all quantum states if and only if it holds for all  $\rho, \sigma \in \mathcal{L}_s(\mathbb{C}^d)$  such that  $\text{tr} \rho = \text{tr} \sigma = 1$ . Thus, by linearity, we can extend this condition to arbitrary Hermitian operators by writing it equivalently as

$$(3) \quad \langle p_\Pi(A) - \text{tr} A c_\Pi, p_\Pi(B) - \text{tr} B c_\Pi \rangle = \alpha(A - (\text{tr} A/d)I | B - (\text{tr} B/d)I) \quad \text{for all } A, B \in \mathcal{L}_s(\mathbb{C}^d).$$

Transforming the lhs, we get

$$\begin{aligned} \langle p_\Pi(A) - \text{tr} A c_\Pi, p_\Pi(B) - \text{tr} B c_\Pi \rangle &= \sum_{i=1}^n (\text{tr}(A \Pi_i) - \text{tr} A \text{tr} \Pi_i/d) (\text{tr}(B \Pi_i) - \text{tr} B \text{tr} \Pi_i/d) \\ &= \sum_{i=1}^n \text{tr} [(A - (\text{tr} A/d)I)(\Pi_i - (\text{tr} \Pi_i/d)I)] \text{tr} [(B - (\text{tr} B/d)I)(\Pi_i - (\text{tr} \Pi_i/d)I)] \\ &= \sum_{i=1}^n (A - (\text{tr} A/d)I | \pi_0(\Pi_i)) (\pi_0(\Pi_i) | B - (\text{tr} B/d)I) \\ &= (A - (\text{tr} A/d)I | S | B - (\text{tr} B/d)I), \end{aligned}$$

where  $S := \sum_{i=1}^n |\pi_0(\Pi_i))(\pi_0(\Pi_i)|$ . Thus (3) is equivalent to

$$(4) \quad (A | S | B) = \alpha(A | B) \quad \forall A, B \in \mathcal{L}_s^0(\mathbb{C}^d),$$

which is equivalent to  $\pi_0(\Pi)$  being a tight operator frame in  $\mathcal{L}_s^0(\mathbb{C}^d)$  with the frame bound  $\alpha$ . In order to calculate  $\alpha$ , let us take the trace on both sides of the equation

$$(5) \quad \sum_{i=1}^n |\pi_0(\Pi_i))(\pi_0(\Pi_i)| = \alpha \mathcal{I}_0,$$

where  $\mathcal{I}_0$  denotes the identity superoperator on  $\mathcal{L}_s^0(\mathbb{C}^d)$ . On the rhs we get  $\alpha(d^2 - 1)$ , since  $\dim \mathcal{L}_s^0(\mathbb{C}^d) = d^2 - 1$ . On the lhs we get

$$\begin{aligned} \sum_{i=1}^n (\pi_0(\Pi_i) | \pi_0(\Pi_i)) &= \sum_{i=1}^n \left[ (\Pi_i | \Pi_i) - \frac{\text{tr} \Pi_i}{d} (I | \Pi_i) - \frac{\text{tr} \Pi_i}{d} (\Pi_i | I) + \frac{(\text{tr} \Pi_i)^2}{d^2} (I | I) \right] \\ &= \sum_{i=1}^n \text{tr} \Pi_i^2 - \frac{1}{d} \sum_{i=1}^n (\text{tr} \Pi_i)^2, \end{aligned}$$

which completes the proof.  $\square$

The condition of  $\pi_0(\Pi)$  being a tight operator frame in  $\mathcal{L}_s^0(\mathbb{C}^d)$  brings to mind the definition of a tight IC-POVM given by Scott in [69]. Let us introduce the following notation:  $P_i := \Pi_i / \text{tr} \Pi_i$ ,  $P := \{P_i\}_{i=1}^n$  and  $\mathcal{F} := \sum_{i=1}^n \text{tr} \Pi_i |P_i)(P_i| = \sum_{i=1}^n \frac{1}{\text{tr} \Pi_i} |\Pi_i)(\Pi_i|$ .

**Definition 4.**  $\Pi$  is a *tight IC-POVM* if  $\pi_0(P)$  is a tight operator frame with respect to the trace measure  $\tau$  ( $\tau(i) = \text{tr} \Pi_i$ ,  $i = 1, \dots, n$ ) in  $\mathcal{L}_s^0(\mathbb{C}^d)$ , i.e. if there exists  $\beta > 0$  such that

$$\sum_{i=1}^n \text{tr} \Pi_i |\pi_0(P_i))(\pi_0(P_i)| = \beta \mathcal{I}_0.$$

*Remark 2.* The definition of a tight IC-POVM can be expressed equivalently in the following way:

$$\mathcal{F} = \beta \mathcal{I} + \frac{1 - \beta}{d} |I)(I|,$$

where  $\mathcal{I}$  stands for the identity superoperator on  $\mathcal{L}_s(\mathbb{C}^d)$ . Note that  $\beta$  can be calculated by taking the trace on both sides of one of the above equations:

$$\beta = \frac{1}{d^2 - 1} \left( \sum_{i=1}^n \frac{\text{tr}\Pi_i^2}{\text{tr}\Pi_i} - 1 \right).$$

Applying Theorem 3 we get the following statement as a simple observation.

**Corollary 4.** *Let  $\Pi$  be a POVM consisting of effects of equal trace. Then  $\Delta_\Pi$  is similar to the quantum state space if and only if  $\Pi$  is a tight IC-POVM. The square of similarity ratio  $\alpha$  is then equal to  $\frac{1}{d^2-1} \left( \sum_{j=1}^n \text{tr}\Pi_j^2 - \frac{d}{n} \right)$ .*

#### 4. THE PROBABILITY RANGE OF 2-DESIGN POVMs

**Definition 5.** We say that  $\{\rho_j\}_{j=1}^n \subset \mathcal{P}(\mathbb{C}^d)$  is a  $t$ -design if

$$\frac{1}{n^2} \sum_{j,k=1}^n f(\text{tr}(\rho_j \rho_k)) = \iint_{(\mathcal{P}(\mathbb{C}^d))^2} f(\text{tr}(\rho\sigma)) d\mu(\rho) d\mu(\sigma)$$

holds for every  $f : \mathbb{R} \rightarrow \mathbb{R}$  polynomial of degree  $t$  or less, where by  $\mu$  we mean the unique unitarily invariant measure on  $\mathcal{P}(\mathbb{C}^d)$ .

Obviously, any  $t$ -design is also an  $s$ -design for  $s < t$ . Note that  $\{\rho_j\}_{j=1}^n \subset \mathcal{P}(\mathbb{C}^d)$  is a 1-design if and only if  $\{\frac{d}{n}\rho_j\}_{j=1}^n$  is a POVM. Moreover, it is a 2-design if and only if  $\{\frac{d}{n}\rho_j\}_{j=1}^n$  is a tight IC-POVM [69, Prop. 13]. We will refer to such rank-1 POVM as a 2-design POVM. That property allows us to rephrase the definition of a 2-design in a more comprehensible way, namely  $\{\rho_j\}_{j=1}^n \subset \mathcal{P}(\mathbb{C}^d)$  is a 2-design if and only if

$$(6) \quad \tau = (d+1) \sum_{j=1}^n \frac{d}{n} \text{tr}(\tau \rho_j) \rho_j - I$$

for every  $\tau$  such that  $\tau^* = \tau$  and  $\text{tr}\tau = 1$ .

**Corollary 5.** *Let  $\Pi$  be a rank-1 POVM consisting of effects of equal trace. Then  $\mathcal{Q}_\Pi$  is similar to the quantum state space if and only if  $\Pi$  is a 2-design POVM. The square of similarity ratio  $\alpha$  is then equal to  $\frac{d}{n(d+1)}$ .*

From now on we assume that  $\Pi = \{\frac{d}{n}\rho_j\}_{j=1}^n$  is a 2-design POVM. For  $\tau \in \mathcal{S}(\mathbb{C}^d)$ ,  $p_j(\tau) := (p_\Pi(\tau))_j = \frac{d}{n} \text{tr}(\tau \rho_j)$  is the probability of obtaining the  $j$ -th outcome. The following equalities are directly derived from (6):

$$(7) \quad \sum_{j=1}^n p_j(\tau) = 1,$$

$$(8) \quad \sum_{j=1}^n (p_j(\tau))^2 = \frac{d(\text{tr}(\tau^2) + 1)}{n(d+1)},$$

$$(9) \quad \sum_{j,k,l=1}^n p_j(\tau) p_k(\tau) p_l(\tau) \text{tr}(\rho_j \rho_k \rho_l) = \frac{\text{tr}(\tau + I)^3}{(d+1)^3}.$$

In particular, for pure states we get

$$(10) \quad \sum_{j=1}^n (p_j(\tau))^2 = \frac{2d}{n(d+1)},$$

$$(11) \quad \sum_{j,k,l=1}^n p_j(\tau) p_k(\tau) p_l(\tau) \text{tr}(\rho_j \rho_k \rho_l) = \frac{d+7}{(d+1)^3}.$$

*Remark 3.* Note that the rhs of the last equation does not depend on  $n$ .

The proof of the following fact can be found in [47].

*Fact 2.* A self-adjoint operator  $\tau$  is a pure quantum state if and only if  $\text{tr}\tau = 1$ ,  $\text{tr}\tau^2 = 1$  and  $\text{tr}\tau^3 = 1$ .

This fact will be helpful for proving the theorem that characterises the probability distributions belonging to  $\mathcal{Q}_{\Pi}^1$ . Note that the statement is more general than [37, Cor. 2.3.4].

**Theorem 6.** *Let  $\Pi = \{\frac{d}{n}\rho_j\}_{j=1}^n$  be a 2-design POVM. Then  $(p_1, \dots, p_n) \in \mathcal{Q}_{\Pi}^1$  if and only if*

- i.  $\frac{n}{d}p_l = (d+1) \sum_{j=1}^n p_j \text{tr}(\rho_j \rho_l) - 1$  for  $l = 1, \dots, n$ ;
- ii.  $\sum_{j=1}^n p_j^2 = \frac{2d}{n(d+1)}$ ;
- iii.  $\sum_{j,k,l=1}^n p_j p_k p_l \text{tr}(\rho_j \rho_k \rho_l) = \frac{d+7}{(d+1)^3}$ .

*Proof.* We already know that every probability distribution from  $\mathcal{Q}_{\Pi}^1$  satisfies all equalities above. Thus to complete the proof it suffices to show that any vector  $(p_1, \dots, p_n) \in \mathbb{R}^n$  fulfilling equalities (i)-(iii) belongs to  $\mathcal{Q}_{\Pi}^1$ . Let us define  $\tau := (d+1) \sum_{j=1}^n p_j \rho_j - I$ . Then

$$\text{tr}(\tau \rho_l) = (d+1) \sum_{j=1}^n p_j \text{tr}(\rho_j \rho_l) - \text{tr}(\rho_l) = \frac{n}{d} p_l$$

and thus  $p_l = \frac{d}{n} \text{tr}(\tau \rho_l)$ . It is now enough to show that  $\tau \in \mathcal{P}(\mathbb{C}^d)$ . Obviously  $\tau^* = \tau$ . Using (i), we show that the numbers  $p_1, p_2, \dots, p_n$  sum up to 1:

$$\sum_{l=1}^n p_l = \frac{d}{n} \left( (d+1) \sum_{j=1}^n p_j \text{tr} \left( \rho_j \sum_{l=1}^n \rho_l \right) - n \right) = \frac{d}{n} (d+1) \frac{n}{d} \sum_{j=1}^n p_j - \frac{d}{n} n = (d+1) \sum_{j=1}^n p_j - d,$$

which gives us  $\sum_{l=1}^n p_l = 1$ . In consequence,  $\text{tr} \tau = (d+1) \sum_{j=1}^n p_j \text{tr}(\rho_j) - d = 1$ . Since (8) and (9) hold true for any Hermitian operator with trace equal to 1, we can compare them with our assumptions concerning the sum of squares and triple products respectively to obtain  $\text{tr} \tau^2 = \text{tr} \tau^3 = 1$ , which completes the proof.  $\square$

Let us take a closer look at equations (i)-(iii) from Theorem 6. As we already know from Corollary 5, they need to describe a  $(2d-2)$ -dimensional submanifold of the  $(d^2-2)$ -dimensional sphere. From the proof above we can see that the first  $n$  linear equations (i) define a  $(d^2-1)$ -dimensional affine subspace  $\mathcal{A}$  in  $\mathbb{R}^n$ . It is easy to see that  $\mathcal{A}$  is the affine span of  $\mathcal{Q}_{\Pi}$ . In particular,  $\mathcal{A} \subset \{x \in \mathbb{R}^n : x_1 + \dots + x_n = 1\}$ . The number of equations can be reduced to  $n - (d^2 - 1)$  since the rest of them needs to be linearly dependent. In particular, if  $n = d^2$ , this system of equations reduces to the single equation  $\sum_{j=1}^{d^2} p_j = 1$ . Note that the only 2-design POVMs with  $d^2$  elements are SIC-POVMs, i.e. those with  $\text{tr}(\rho_j \rho_k) = \frac{1}{d+1}$  for  $j \neq k$ . The quadratic form (ii) is obviously the equation of the sphere in  $\mathbb{R}^n$  centred at 0 and of radius  $\sqrt{\frac{2d}{n(d+1)}}$ . The intersection of this sphere with the affine subspace  $\mathcal{A}$  gives us the  $(d^2-2)$ -dimensional sphere we are looking for. Finally, the cubic form (iii) is responsible for cutting the  $(2d-2)$ -dimensional submanifold from the sphere in question. We can now state the following:

**Corollary 7.**

- i. *The set  $\mathcal{Q}_{\Pi}^1$  is fully described by equations (i)-(ii) if and only if  $d = 2$ .*
- ii. *The linear equations (i) can be reduced to a single equation  $\sum_{j=1}^n p_j = 1$  if and only if  $\Pi$  is a SIC-POVM.*

A natural question arises whether we can provide a similar characterization of  $\mathcal{Q}_{\Pi}$  as we did for  $\mathcal{Q}_{\Pi}^1$  in Theorem 6. As we can see, the proof is based on the fact that the pure states are fully described by  $\text{tr} \tau = \text{tr} \tau^2 = \text{tr} \tau^3 = 1$ . The mixed states obviously satisfy  $\text{tr} \tau = 1$  and  $\text{tr} \tau^2 \leq 1$  and it is tempting to write down the third inequality in a similar manner. However, it turns out that in order to provide a complete characterization of  $\tau \in \mathcal{S}(\mathbb{C}^d)$  in terms of  $\text{tr} \tau^k$ , we need additional  $d-2$  inequalities. Put together they take the form  $S_k \geq 0$  ( $k \in \{2, \dots, d\}$ ), where  $S_k$  can be defined recursively by  $S_k = \frac{1}{k} \sum_{j=1}^k (-1)^{j-1} \text{tr}(\tau^j) S_{k-j}$  and  $S_0 = S_1 = 1$  [15]. For example, the condition on  $\text{tr} \tau^3$  is as follows:  $3\text{tr} \tau^2 - 2\text{tr} \tau^3 \leq 1$ . Thus such characterization is possible but it becomes more and more complicated with the growth of  $d$ . However, for  $d = 2, 3$  we can characterise  $\mathcal{Q}_{\Pi}$  in a relatively simple way.

**Corollary 8.** *Let  $\Pi = \{\frac{d}{n}\rho_j\}_{j=1}^n$  be a 2-design POVM. If  $(p_1, \dots, p_n) \in \mathcal{Q}_{\Pi}$ , then*

- i.  $\frac{n}{d}p_l = (d+1) \sum_{j=1}^n p_j \text{tr}(\rho_j \rho_l) - 1$  for  $l = 1, \dots, n$ ;
- ii.  $\sum_{j=1}^n p_j^2 \leq \frac{2d}{n(d+1)}$ ;
- iii.  $\sum_{j,k,l=1}^n p_j p_k p_l \text{tr}(\rho_j \rho_k \rho_l) \geq \frac{9n}{2d(d+1)^2} \sum_{j=1}^n p_j^2 + \frac{d-2}{(d+1)^3}$ .

*Moreover, conditions (i)-(iii) are sufficient for  $d = 3$  and (i)-(ii) are sufficient for  $d = 2$ .*

## 5. EXAMPLES

In the following examples we provide some explicit formulae for the  $(d^2 - 1)$ -dimensional affine subspaces  $\mathcal{A}$  defined by the system of linear equations (i).

**Example 2** (Cubical POVM). Let us consider a cubical POVM  $\Pi = \{\frac{1}{4}\rho_j\}_{j=1}^8$ , i.e. the states  $\rho_1, \dots, \rho_8$  are represented on the Bloch sphere by the vertices of a cube, e.g.  $\frac{1}{\sqrt{6}}(\pm 1, \pm 1, \pm 1)$ . Let us label these vertices in the following way: the vertices of the bottom face are labelled in sequence with 1-4 and if  $i$  and  $j$  are the labels of the opposite vertices, then  $j = i + 4 \pmod{8}$ . The eight linear equations (i) from Theorem 6 reduce to the following  $8 - (2^2 - 1) = 5$  linearly independent ones:

$$\begin{cases} p_1 + p_5 = \frac{1}{4} \\ p_2 + p_6 = \frac{1}{4} \\ p_3 + p_7 = \frac{1}{4} \\ p_4 + p_8 = \frac{1}{4} \\ p_1 + p_3 + p_6 + p_8 = \frac{1}{2}. \end{cases}$$

It is easy to see that the first four of them guarantee that  $p_1 + \dots + p_8 = 1$ . Obviously, the 3-dimensional affine subspace of  $\mathbb{R}^8$  defined by these equations is label-dependent. The number of possible labellings is  $8! = 40320$ . However, two of them produce the same set of equations, if the permutation transforming one to the other corresponds to an isometric operation on the cube. The isometries of the cube are described by the elements of the octahedral group  $O_h$ . Thus the number of different subspaces is  $\frac{8!}{|O_h|} = \frac{40320}{48} = 840$ .

**Example 3** (Cuboctahedral and icosahedral POVMs). The polyhedra defining these POVMs (cuboctahedron and icosahedron) have the same number of vertices:  $n = 12$ , which can be represented on the Bloch sphere by  $\frac{1}{\sqrt{2(s^2+1)}}(\pm s, \pm 1, 0)$ ,  $\frac{1}{\sqrt{2(s^2+1)}}(0, \pm s, \pm 1)$  and  $\frac{1}{\sqrt{2(s^2+1)}}(\pm 1, 0, \pm s)$ , where  $s = 1$  for cuboctahedron and  $s = (1 + \sqrt{5})/2$  (*golden ratio*, usually denoted by  $\varphi$ ) for icosahedron. If we label these vertices as follows:  $v_1 = (+, +, 0)$ ,  $v_3 = (+, -, 0)$ ,  $v_5 = (0, +, +)$ ,  $v_7 = (0, +, -)$ ,  $v_9 = (+, 0, +)$ ,  $v_{11} = (-, 0, +)$  and  $v_{2j} = -v_{2j-1}$  for  $j \in \{1, \dots, 6\}$ , then the different values of the parameter  $s$  result in slightly different affine subspaces defined by the following systems of 9 linear equations:

$$\text{cuboctahedron: } \begin{cases} p_1 + p_2 = \frac{1}{6} \\ p_3 + p_4 = \frac{1}{6} \\ p_5 + p_6 = \frac{1}{6} \\ p_7 + p_8 = \frac{1}{6} \\ p_9 + p_{10} = \frac{1}{6} \\ p_{11} + p_{12} = \frac{1}{6} \\ p_1 - p_3 + p_6 + p_8 = \frac{1}{6} \\ p_5 - p_7 + p_{10} + p_{12} = \frac{1}{6} \\ p_9 - p_{11} + p_2 + p_4 = \frac{1}{6} \end{cases}, \quad \text{icosahedron: } \begin{cases} p_1 + p_2 = \frac{1}{6} \\ p_3 + p_4 = \frac{1}{6} \\ p_5 + p_6 = \frac{1}{6} \\ p_7 + p_8 = \frac{1}{6} \\ p_9 + p_{10} = \frac{1}{6} \\ p_{11} + p_{12} = \frac{1}{6} \\ \varphi(p_1 - p_3) + p_6 + p_8 = \frac{1}{6} \\ \varphi(p_5 - p_7) + p_{10} + p_{12} = \frac{1}{6} \\ \varphi(p_9 - p_{11}) + p_2 + p_4 = \frac{1}{6} \end{cases}.$$

As in the previous case, the definitions of the subspaces are label-dependent. The number of possible labellings is  $12!$ , but taking into account the symmetry groups of cuboctahedron and icosahedron, i.e. the octahedral group  $O_h$  and the icosahedral group  $I_h$ , we get the numbers of different subspaces are  $\frac{12!}{|O_h|} = \frac{12!}{48} = 9979200$  and  $\frac{12!}{|I_h|} = \frac{12!}{120} = 3991680$ .

Starting from dimension  $d = 3$ , the equation of third degree plays a crucial role in defining  $\mathcal{Q}_\Pi^1$ . In the following example we take a closer look at the 1-parameter family of 2-design POVMs for which the equations of first and second degree coincide, but not these of third degree. But first let us observe that the lhs of (iii) in Theorem 6 can be written in a slightly different way if we assume that both (i) and (ii) from the same theorem hold. We start with:

$$\sum_{j,k,l=1}^n p_j p_k p_l \text{tr}(\rho_j \rho_k \rho_l) = \sum_{j=1}^n p_j^3 \text{tr}(\rho_j^3) + 3 \sum_{\substack{j \neq k \\ 8}} p_j^2 p_k \text{tr}(\rho_j^2 \rho_k) + \sum_{j \neq k \neq l \neq j} p_j p_k p_l \text{tr}(\rho_j \rho_k \rho_l).$$

But  $\rho_j^2 = \rho_j$  and  $\text{tr}(\rho_j^3) = 1$ . Moreover,

$$\begin{aligned} \sum_{j \neq k} p_j^2 p_k \text{tr}(\rho_j \rho_k) &= \sum_{j=1}^n p_j^2 \left( \sum_{k=1}^n p_k \text{tr}(\rho_j \rho_k) - p_j \text{tr}(\rho_j^2) \right) = \sum_{j=1}^n p_j^2 \left( \frac{1}{d+1} \left( \frac{n}{d} p_j + 1 \right) - p_j \right) \\ &= \left( \frac{n}{d(d+1)} - 1 \right) \sum_{j=1}^n p_j^3 + \frac{1}{d+1} \sum_{j=1}^n p_j^2 = \left( \frac{n}{d(d+1)} - 1 \right) \sum_{j=1}^n p_j^3 + \frac{2d}{n(d+1)^2}. \end{aligned}$$

Thus, the third degree equation now takes the form:

$$(12) \quad \left( \frac{3n}{d(d+1)} - 2 \right) \sum_{j=1}^n p_j^3 + \sum_{j \neq k \neq l \neq j} p_j p_k p_l \text{tr}(\rho_j \rho_k \rho_l) = \frac{n(d+7) - 6d(d+1)}{n(d+1)^3}$$

**Example 4** (SIC-POVMs in dimension 3). Let

$$v_{0,j}^t = \frac{1}{\sqrt{2}}(-e^{it}\eta^j, 0, 1), \quad v_{1,j}^t = \frac{1}{\sqrt{2}}(1, -e^{it}\eta^j, 0), \quad v_{2,j}^t = \frac{1}{\sqrt{2}}(0, 1, -e^{it}\eta^j),$$

where  $\eta = e^{2\pi i/3}$ ,  $j \in \{0, 1, 2\}$  and  $t \in [0, \pi/3)$ . Then  $\Pi^t := \{\frac{1}{3}\rho_{m,j}^t\}_{m,j=0}^2 := \{\frac{1}{3}|v_{m,j}^t\rangle\langle v_{m,j}^t|\}_{m,j=0}^2$  is a SIC-POVM and for  $t \neq t'$  the sets  $\Pi^t$  and  $\Pi^{t'}$  are not unitarily equivalent. It is easy to see that the equations of first and second degree are the same for every  $t$ , but that is not the case for the third degree equation. Let us introduce the following notation:

$$\begin{aligned} J &:= \{(\alpha, \beta, \gamma) \in (\mathbb{Z}_3 \times \mathbb{Z}_3)^3 | \alpha \neq \beta \neq \gamma \neq \alpha\} \\ J_k &:= \{(\alpha, \beta, \gamma) \in (\mathbb{Z}_3 \times \mathbb{Z}_3)^3 | \alpha_1 \neq \beta_1 \neq \gamma_1 \neq \alpha_1, \alpha_2 + \beta_2 + \gamma_2 = k \pmod{3}\}, \quad k = 0, 1, 2 \\ J_3 &:= \{(\alpha, \beta, \gamma) \in (\mathbb{Z}_3 \times \mathbb{Z}_3)^3 | \alpha_1 = \beta_1 = \gamma_1, \alpha_2 \neq \beta_2 \neq \gamma_2 \neq \alpha_2\} \\ J' &:= J \setminus (J_0 \cup J_1 \cup J_2 \cup J_3). \end{aligned}$$

Now, using (12), we get (for the sake of clarity we omit the label  $t$ )

$$\begin{aligned} \frac{1}{32} &= \frac{1}{4} \sum_{\alpha \in \mathbb{Z}_3 \times \mathbb{Z}_3} p_\alpha^3 + \sum_{(\alpha, \beta, \gamma) \in J} p_\alpha p_\beta p_\gamma \text{tr}(\rho_\alpha \rho_\beta \rho_\gamma) \\ &= \frac{1}{4} \sum_{\alpha \in \mathbb{Z}_3 \times \mathbb{Z}_3} p_\alpha^3 - \frac{1}{8} \cos(3t) \sum_{(\alpha, \beta, \gamma) \in J_0} p_\alpha p_\beta p_\gamma + \frac{1}{16} (\cos(3t) + \sqrt{3} \sin(3t)) \sum_{(\alpha, \beta, \gamma) \in J_1} p_\alpha p_\beta p_\gamma \\ &\quad + \frac{1}{16} (\cos(3t) - \sqrt{3} \sin(3t)) \sum_{(\alpha, \beta, \gamma) \in J_2} p_\alpha p_\beta p_\gamma - \frac{1}{8} \sum_{(\alpha, \beta, \gamma) \in J_3} p_\alpha p_\beta p_\gamma + \frac{1}{16} \sum_{(\alpha, \beta, \gamma) \in J'} p_\alpha p_\beta p_\gamma \end{aligned}$$

For  $t = 0$  we get the Hesse configuration and the above equation takes a particularly nice form [76]:

$$\sum_{\alpha \in \mathbb{Z}_3 \times \mathbb{Z}_3} p_\alpha^3 - \frac{1}{2} \sum_{(\alpha, \beta, \gamma) \in J_0 \cup J_3} p_\alpha p_\beta p_\gamma = 0.$$

## 6. MUB-LIKE POVMs

**6.1. MUBs.** Another remarkable example of a 2-design POVM is a *complete set of mutually unbiased bases (MUBs)* in  $\mathbb{C}^d$ , where  $d$  is a prime power. (The question whether complete sets of MUBs exist in other dimensions remains open). Such POVM  $\Pi$  consists of  $d(d+1)$  effects of the form  $\frac{1}{d+1}\rho_j$ , where  $\rho_j \in \mathcal{P}(\mathbb{C}^d)$  for  $j = 1, 2, \dots, d(d+1)$ , and

$$\text{tr}(\rho_{kd+l} \rho_{k'd+l'}) = \begin{cases} 1 & \text{for } k = k', l = l' \\ 0 & \text{for } k = k', l \neq l' \\ \frac{1}{d} & \text{for } k \neq k' \end{cases}$$

for  $k, k' \in \{0, \dots, d\}$  and  $l, l' \in \{1, \dots, d\}$ .

The fact that a complete set of MUBs constitutes a 2-design POVM was first shown explicitly in [49], however, this also follows easily [5] from the fact that in this case  $\Pi$  fulfils both the *Welch bound* [81] and the *Levenshtein bound* [52] for the angles between 2-design lines.

Now, the system of linear equations defining the primal affine space  $\mathcal{A}$  takes a particularly nice form since instead of the initial  $n = d(d+1)$  equations it suffices to consider the following  $d+1$  equations

expressing the simple fact that the probabilities over any basis ( $k = 0, \dots, d$ ) need to sum up to  $\frac{1}{d+1}$ :

$$\sum_{l=1}^d p_{kd+l} = \frac{1}{d+1}.$$

We shall show that this result is valid even in more general settings, see Theorem 9 below.

**6.2. MUB-like 2-designs: definition and the orthogonality graph.** Let us consider a 2-design POVM  $\Pi = \{\frac{d}{n}\rho_j\}_{j=1}^n$ , where  $\rho_j \in \mathcal{P}(\mathbb{C}^d)$  for  $j = 1, \dots, n$ . We call  $\Pi$  *MUB-like* [46] iff there exists  $a > 0$  such that  $\{\text{tr}(\rho_j\rho_k) : j, k = 1, \dots, n, j \neq k\} = \{0, a\}$ . The *orthogonality graph* for  $\Pi$  is the graph  $\Gamma$  with the vertex set  $\{\rho_j\}_{j=1}^n$  and the adjacency relation defined by  $\rho \sim \sigma$  iff  $\rho \perp \sigma$  iff  $\text{tr}(\rho\sigma) = 0$ . Now, we can apply the results of Hoggar, who, in even more general setting, examined the properties of  $\Gamma$  [43, Theorem 5.2] [45, Sec. 3], employing the unpublished notes of Neumaier [56]. In particular, he showed that  $\Gamma$  is a distance regular graph with diameter 2, and so strongly regular, see [11]. We now specify Hoggar's results for MUB-like 2-design POVMs. (Note, however, that Hoggar analysed the graph complementary to  $\Gamma$ .) Denote by:

- $\varkappa$  - the number of vertices of  $\Gamma$  adjacent (orthogonal) to a given vertex;
- $\lambda$  (resp.  $\mu$ ) - the number of vertices of  $\Gamma$  adjacent to a pair of adjacent (resp. not adjacent) vertices.

Obviously,  $\Gamma$  is non-complete and connected unless  $\mu = 0$ . The adjacency matrix of  $\Gamma$  has three eigenvalues  $\varkappa$ ,  $r$ , and  $-q$ , where  $r, q \in \mathbb{N}$ ,  $1 \leq q \leq r^2$ ,  $\psi := \frac{r(q-1)}{r+q} \in \mathbb{N}$ , with the multiplicities 1,  $f$ , and  $g$ , respectively. Note that the inequality  $q \leq r^2$  follows from the Delsarte-Goethals-Seidel bound [27], see also [53, Theorem 7.2], for the cardinality of sets of lines in  $\mathbb{C}^d$  having a prescribed number of angles. Moreover,  $a = \frac{1}{r+1}$ , and

$$\begin{aligned} d &= r + \psi + 1, & n &= d(r + 2q), \\ \varkappa &= (d - 1)q, & \mu &= \psi q, & \lambda &= \mu + r - q, \\ f &= n - d^2, & g &= d^2 - 1. \end{aligned}$$

Clearly,  $\Pi$  saturates both the Welch bound and the Levenshtein bound, which are in this case equivalent as

$$(13) \quad a = \frac{2n - d(d+1)}{(n-d)(d+1)}.$$

In fact, if  $\Pi$  is a rank-one POVM consisting of effects of equal trace such that  $\{\text{tr}(\rho_j\rho_k) : j, k = 1, \dots, n, j \neq k\} = \{0, a\}$ , then  $\Pi$  forms a 2-design if and only if (13) holds [28, Proposition 3].

Clearly, a maximal clique (full subgraph) in  $\Gamma$ , i.e., a maximal orthogonal set, has at most  $d$  elements, which is just the Hoffman-Delsarte bound for  $\Gamma$  [71], as  $1 + \varkappa/q = d$ . Let us recall that a clique  $C$  is called *regular* if every point not in  $C$  is adjacent to the same number (the *nexus*) of points in  $C$ . It follows from [57, Theorem 1.1, Corollary 1.2] that all regular cliques in  $\Gamma$ , if exist, have  $d$  elements (and so they are so called *Delsarte cliques*) with the nexus equal to  $\psi$ . From [71, Theorem 3.1.iv] we deduce that every clique in  $\Gamma$  of size  $d$  is regular. Hence,  $\Gamma$  is a *Delsarte clique graph* (for definition see [4]) if and only if for every  $j, k = 1, \dots, n, j \neq k$  such that  $\rho_j \perp \rho_k$ ,  $\{\rho_j, \rho_k\}$  is contained in the same number (say  $c$ ) of bases. More precisely,  $\Gamma$  is then a Delsarte clique graph with parameters  $(\varkappa, d - 1, c)$ . Moreover, double counting argument shows that the number of maximal cliques in every local graph is  $cq$ , and the number of maximal cliques in  $\Gamma$  is  $(r + 2q)cq$ . Note that if  $\Gamma$  is an *edge transitive graph* and there is a Delsarte clique in  $\Gamma$ , then  $\Gamma$  is a Delsarte clique graph. In particular, this is true for *rank 3 graphs*, i.e. strongly regular graphs generated by a *rank 3 permutation group* of even order acting on a finite set  $X$  (i.e., a group with exactly three orbits on  $X \times X$ ), as they are edge transitive [41].

**6.3. Examples.** Let us now consider two extreme cases:  $q = 1$  and  $q = r^2$ , where  $n$  is, resp., minimal and maximal, for a given  $d$ .

- $q = 1$  (iff  $\psi = 0$ )

In this case  $a = \frac{1}{d}$ ,  $n = d(d+1)$ ,  $\varkappa = d - 1$ ,  $\lambda = d - 2$  and  $\mu = 0$ . In consequence,  $\Pi$  must be a *complete set of mutually unbiased bases (MUBs)*.

- $q = r^2$  (iff  $\psi = r - 1$ )

Then  $d = 2r$ ,  $a = \frac{1}{r+1}$ ,  $n = 2r^2(2r+1) = d^2(d+1)/2$ ,  $\varkappa = (2r-1)r^2$ ,  $\lambda = (r-1)^2 r$  and  $\mu = (r-1)r^2$ . Hoggar showed [45, Theorem 3.7] that this is also a sufficient and necessary condition for  $\Pi$  to be a (minimal or tight) 3-*design*. Note that  $\Pi$  cannot be a 4-*design* [43, Theorem 5.2].

Note that the case  $q = r = 1$ , i.e., the POVM consisting of 3 MUBs in dimension  $d = 2$  that form the regular octahedron inscribed in the Bloch sphere, lies at the intersection of these two extremes. Besides complete sets of MUBs, which exist for every prime power  $d$ , but not necessarily for other dimensions, we know four other MUB-like POVMs, one in each of dimensions 4, 5, 6 and 28, see also [28]. The parameters of these POVMs and their orthogonality graphs are collected in Tab. 1.

$n$	$\varkappa$	$\lambda$	$\mu$	$d$	$r$	$q$	$\psi$	$c$
$d(d+1)$	$d-1$	$d-2$	0	$d$	$d-1$	1	0	1
40	12	2	4	4	2	4	1	1
45	12	3	3	5	3	3	1	1
126	45	12	18	6	3	9	2	3
4060	1755	730	780	28	15	65	12	45

TABLE 1. Parameters of the orthogonality graphs generated by MUB-like POVMs.

Note that all these graphs are Delsarte clique graphs:

- For MUBs  $\Gamma$  is the disjoint union of maximal cliques and, in consequence, a Delsarte clique graph with  $\psi = 0$  and  $c = 1$ .
- $d = 4$  [43, Ex. 7]. This 3-*design* was introduced in [61, Sec. 6] under the name of *Penrose dodecahedron*, see also [54,62,83], and, independently, as the diameters of the *Witting polytope* [19, 20]. Waegell and Aravind [78] showed that these two constructions are in fact equivalent. Hoggar [44] proved that in this case  $\Gamma$  is the collinearity graph of one of two generalised *quadrangles of order (3, 3)* [59] [60, Sec. 3.1.1, 6.2.1], namely  $W(3)$  arising as the set of absolute points and lines of a symplectic polarity of projective geometry  $PG(3, 3)$ , see also [12, Ex. 10.10]. Hence  $\Gamma$  is a (rank 3) Delsarte clique graph with  $\psi = 1$  and  $c = 1$ .
- $d = 5$  [43, Ex. 18] This 2-*design* was defined in [27] and it is equal to the *line system*  $\mathcal{K}_5$  [53, p.107 & 166]. We shall show below (Ex. 5) that in this case  $\Gamma$  is the collinearity graph of the unique *generalised quadrangle of order (4, 2)* [42] [12, Ex. 10.11]. In consequence,  $\Gamma$  is a (rank 3) Delsarte clique graph with  $\psi = 1$  and  $c = 1$ .
- $d = 6$  [43, Ex. 7] This 3-*design* was introduced in [55] and it is just the *line system*  $\mathcal{K}_6$  [53, p.107 & 166]. The orthogonality graph for this design is a unique rank 3 strongly regular graph with parameters (126, 45, 12, 18) [8] [12, Ex. 10.32], having the collinearity graph of unique quadrangle of order (4, 2), see above, as its local graph [21, Sec. 5.2]. Hence,  $\Gamma$  is a (rank 3) Delsarte clique graph with  $\psi = 2$  and  $c = 3$ .
- $d = 28$  [43, Ex. 20] This MUB-like 2-*design* (with  $a = 1/16$ ) was defined in [18] and it comes from a 28-dimensional representation of the sporadic simple Rudvalis group. This group is a rank 3 permutation group of even order [41] on a 4060-element set and, as such, it generates an edge transitive strongly regular (*Rudvalis*) *graph*, which is the orthogonality graph for the 2-*design*. Now,  $\Gamma$  is a (rank 3) Delsarte clique graph with  $\psi = 12$  and  $c = 45$  [12, Ex. 10.65].

*Problem 1.* Let  $\Pi$  be a MUB-like POVM. Is it true that its orthogonality graph is always a Delsarte clique graph?

The next result gives us an alternative description of the primal affine space  $\mathcal{A}$  introduced after Theorem 6, and ipso facto an alternative form of the particular case of the primal equation (‘Urgleichung’) in the MUB-like case, assuming that the orthogonality graph  $\Gamma$  is a Delsarte clique graph. On the other hand, it shows that the primal polytope (see Section 7)  $\mathcal{A} \cap \Delta_n = \frac{d}{n} \cdot \text{QSTAB}(\Gamma) \cap \Delta_n$ , where  $\text{QSTAB}(\Gamma)$  is the *clique constrained stable set polytope* for  $\Gamma$  [1].

#### 6.4. Main result.

**Theorem 9.** *Let  $\Pi$  be a MUB-like POVM and let its orthogonality graph be a Delsarte clique graph. Denote by  $\mathcal{C}$  the set of orthogonal bases (maximal cliques) contained in  $\{\rho_j\}_{j=1}^n$ . For  $C \in \mathcal{C}$  set  $J_C := \{j = 1, \dots, n : \rho_j \in C\}$ . Then the following conditions are equivalent for  $p \in (\mathbb{R}^+)^n$ :*

- (1)  $p$  fulfils (i) from Theorem 6;
- (2)  $p \in \Delta_n$  and for every  $C \in \mathcal{C}$

$$(14) \quad \sum_{j \in J_C} p_j = \frac{d}{n};$$

- (3)  $p \in \Delta_n$  and for every clique  $C$  in  $\Gamma$

$$(15) \quad \sum_{j \in J_C} p_j \leq \frac{d}{n}.$$

*Proof.* For  $l = 1, \dots, n$  denote by  $\mathcal{C}_l := \{C \in \mathcal{C} : \rho_l \in C\}$ ,  $A_l := \{j = 1, \dots, n : \text{tr}(\rho_j \rho_l) = a\}$  and  $O_l := \{j = 1, \dots, n : \text{tr}(\rho_j \rho_l) = 0\}$ . Note that  $|\mathcal{C}_l| = cq$ .

The implication (2)  $\Rightarrow$  (3) follows from the fact that each clique is contained in a maximal one.

To show (3)  $\Rightarrow$  (1), set  $l = 1, \dots, n$ . Applying (15), we get

$$\sum_{C \in \mathcal{C}_l} \sum_{j \in J_C} p_j \leq cq \frac{d}{n}.$$

In consequence,

$$cqp_l + c \sum_{j \in O_l} p_j = cqp_l + \sum_{C \in \mathcal{C}_l} \left( \sum_{j \in J_C} p_j - p_l \right) \leq cq \frac{d}{n},$$

and so

$$(16) \quad qp_l + \sum_{j \in O_l} p_j \leq q \frac{d}{n}.$$

Multiplying both sides of (16) by  $(d+1)a$ , we get

$$\begin{aligned} \frac{n}{d} p_l - (d+1)(p_l + a \sum_{j \in A_l} p_j) + \frac{r+2q}{r+q} &= (d+1)(aq + (1-a))p_l - (d+1)(p_l + a \sum_{j \in A_l} p_j) + (d+1)a \\ &= (d+1)aqp_l + (d+1)a(1-p_l - \sum_{j \in A_l} p_j) \\ &= (d+1)a(qp_l + \sum_{j \in O_l} p_j) \\ &\leq (d+1)aq \frac{d}{n} = \frac{q}{r+q}. \end{aligned}$$

Thus,

$$(17) \quad \frac{n}{d} p_l \leq (d+1)(p_l + a \sum_{j \in A_l} p_j) - 1.$$

On the other hand, the sums of both sides of (17) over  $n = 1, \dots, l$  are equal as

$$\sum_{l=1}^n ((d+1)(p_l + a \sum_{j \in A_l} p_j) - 1) = (d+1)(1 + a(n - \varkappa - 1)) - n = \frac{n}{d} = \frac{n}{d} \sum_{l=1}^n p_l.$$

Hence, (1) follows.

To show (1)  $\Rightarrow$  (2), we note first that summing the equalities in (1) over  $n = 1, \dots, l$  we get

$$\sum_{l=1}^n p_l = \frac{(d+1)a(n - \varkappa - 1) - n}{\frac{n}{d} - (d+1)} = 1.$$

Now fix  $C \in \mathcal{C}$ . Then

$$\begin{aligned} \frac{n}{d} \sum_{l \in C} p_l &= (d+1) \left( \sum_{l \in C} p_l + a \sum_{l \in C} \sum_{j \in A_l} p_j \right) - d \\ &= (d+1) \sum_{l \in C} p_l + a(d+1)(d-\psi) \left( 1 - \sum_{l \in C} p_l \right) - d \\ &= (d+1) \sum_{l \in C} p_l + (d+1) \left( 1 - \sum_{l \in C} p_l \right) - d, \end{aligned}$$

and so (14) holds, which completes the proof.  $\square$

**Example 5** (Two-distance 2-design in dimension 5). This 2-design consists of 45 projections onto vectors  $(1, 0, 0, 0, 0)$  and  $\frac{1}{4}(0, 1, \pm\eta, \pm\eta, \pm 1)$  under all cyclic permutations of their coordinates, where  $\eta := e^{2\pi i/3}$ . The 2-design POVM is then formed by rescaling these projections by  $\frac{5}{45} = \frac{1}{9}$ . The inner products between different states of this 2-design take the values 0 and  $\frac{1}{4}$ . As a two-distance 2-design, it carries a strongly regular graph  $\text{srg}(45, 12, 3, 3)$ . It turns out that among 78 non-isomorphic strongly regular graphs with such parameters, our graph is the one generated by the point graph of the generalised quadrangle of order  $(4, 2)$ , meaning that the 45 vectors constituting the 2-design can be arranged into 27 orthonormal bases in such a way that every vector belongs to 3 bases, every 2 vectors belong to at most 1 basis, and for every vector  $v$  and every base  $B$  such that  $v \notin B$  there exist a unique vector  $v'$  and a basis  $B'$  such that  $v' \in B'$ ,  $v \in B'$  and  $v' \in B$ , see Fig. 2 (adapted from [64, p. 61] and [68, Fig. 1]). Obviously, the sum of the probabilities over any basis is equal to  $\frac{1}{9}$ . But there are 27 bases and we need just  $45 - (25 - 1) = 21$  linear equations to describe the affine space  $\mathcal{A}$ . An example of how to get rid of 6 equations (respective bases are marked in blue) in order to obtain a system of 21 linearly independent equations is presented in Fig. 2.

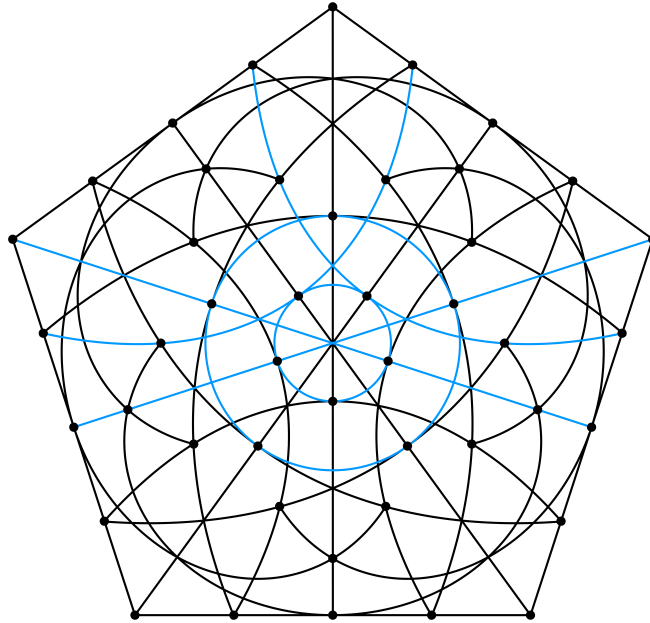


FIGURE 2. Two-distance 2-design in  $\mathbb{C}^5$  as  $\text{GQ}(4, 2)$ . Vertices represent vectors and curves (lines, circles or arcs of ellipses) represent bases. Sums of probabilities over each of blue bases can be omitted in the description of the primal affine subspace  $\mathcal{A}$ .

## 7. GEOMETRIC PROPERTIES OF GENERALISED QPLEX

To understand a geometric picture hidden behind the algebraic equations presented in the previous sections, let us consider a 2-design POVM  $\Pi = \{\frac{d}{n}\rho_j\}_{j=1}^n$ , where  $\{\rho_j\}_{j=1}^n \subset \mathcal{P}(\mathbb{C}^d)$ . We show that the geometry of generalised qplex generated by this design is quite similar to that of (Hilbert) qplex, in spite

of the fact that now this object is not located between two simplices but between two dual polytopes lying in a medial cross-section of the probability simplex by an affine space. Also our approach is quite similar to that presented in [2] although some alterations were necessary.

Let us recall that from Corollary 5 it follows that the measurement map  $p_\Pi : \mathcal{S}(\mathbb{C}^d) \rightarrow \mathcal{Q}_\Pi$  is a similarity of ratio  $d^{1/2}m$ , where  $m := n^{-1/2}(d+1)^{-1/2}$ . Clearly, the *uniform distribution*  $c_n := (1/n, \dots, 1/n) = p_\Pi(I/d) \in \mathcal{Q}_\Pi$ . We know that the maximal ball centred at  $I/d$  and contained in  $\mathcal{S}(\mathbb{C}^d)$  has radius  $(d(d-1))^{-1/2}$ . Hence the maximal ball centred at  $c_n$  and contained in  $\mathcal{Q}_\Pi$  has radius  $r := m(d-1)^{-1/2}$ . On the other hand,  $\mathcal{S}(\mathbb{C}^d)$  is contained in the ball with centre  $I/d$  and radius  $((d-1)/d)^{1/2}$  with the pure states contained in the corresponding sphere. Thus  $\mathcal{Q}_\Pi$  is contained in the ball centred at  $c_n$  with radius  $R := m(d-1)^{1/2}$  and  $\mathcal{Q}_\Pi^1$  is contained in the corresponding sphere. In short,

$$(18) \quad B_{\mathcal{A}}(c_n, r) \subset \mathcal{Q}_\Pi \subset B_{\mathcal{A}}(c_n, R) \quad \text{and} \quad \mathcal{Q}_\Pi^1 \subset \partial B_{\mathcal{A}}(c_n, R).$$

For  $j = 1, \dots, n$  introduce the *basis distributions* given by  $f_j := p_\Pi(\rho_j)$  generating the *basis polytope*

$$D := \text{conv}\{f_j : j = 1, \dots, n\}.$$

Note that the *uniform distribution*  $c_n := (1/n, \dots, 1/n) = p_\Pi(\frac{1}{d}I) = p_\Pi(\frac{1}{n}\sum_{j=1}^n \rho_j) \in D$ , and  $(f_j)_k = (f_k)_j$  for  $j, k = 1, \dots, n$ .

*Fact 3.*  $B_{\mathcal{A}}(c_n, R)$  is the circumscribed ball of  $D$ .

Immediately from Theorem 6 we get  $\mathcal{A}$  is the affine span of  $D$  in  $\mathbb{R}^n$ . Now, the following statement is the result of simple computation.

*Fact 4.* Let  $p \in \mathbb{R}^n$ . The following conditions are equivalent:

- i.  $p \in \mathcal{A}$ ;
- ii.  $p = (d+1)\sum_{j=1}^n p_j f_j - d c_n$ ;
- iii.  $p - c_n = (d+1)\sum_{j=1}^n p_j (f_j - c_n)$ ;
- iv.  $\frac{1}{d+1}\langle p, e_k \rangle = \langle p, f_k \rangle - d m^2$  for every  $k = 1, \dots, n$ ;
- v.  $p - c_n \perp e_k - (d+1)(f_k - c_n)$  for every  $k = 1, \dots, n$ .

Note that (ii) is just the famous *primal equation* ('*Urgleichung*') introduced by the founders of quantum Bayesianism and applied to the repeated 'standard' measurement  $\Pi$ .

Let us now consider the homothety in  $\mathcal{A}$  with the centre at  $c_n$  and the ratio equal to  $1/(d+1)$ , i.e. the map  $h : \mathcal{A} \rightarrow \mathcal{A}$  given by

$$h(p) := c_n + \frac{p - c_n}{d+1} = \frac{1}{d+1}p + \frac{d}{d+1}c_n$$

for  $p \in \mathcal{A}$ . Let  $P_{\mathcal{A}} : \mathbb{R}^n \rightarrow \mathcal{A}$  denote the orthogonal projection on  $\mathcal{A}$ .

*Fact 5.* In the above situation  $h(P_{\mathcal{A}}e_k) = f_k$  for every  $k = 1, \dots, n$ . In particular,  $h(P_{\mathcal{A}}\Delta_n) = D$ .

*Proof.* Let  $k = 1, \dots, n$ . Then it follows from condition (v) in Fact 4 that  $P_{\mathcal{A}}e_k = c_n + (d+1)(f_k - c_n)$ . Hence  $h(P_{\mathcal{A}}e_k) = f_k$ , as desired.  $\square$

Define the *primal polytope*  $\Delta$  as the cross-section of  $\Delta_n$  by  $\mathcal{A}$ , i.e.

$$\Delta := \mathcal{A} \cap \Delta_n.$$

It follows from Theorem 6 that

$$D \subset \mathcal{Q}_\Pi \subset \Delta.$$

Thus

$$D \cup B_{\mathcal{A}}(c_n, r) \subset \mathcal{Q}_\Pi \subset \Delta \cap B_{\mathcal{A}}(c_n, R).$$

**Theorem 10.** *The above cross-section is medial, i.e. the vertices of  $\Delta_n$  are equidistant from  $\mathcal{A}$ . More precisely,*

$$\text{dist}(e_k, \mathcal{A}) = 1 - \frac{d^2}{n}$$

for every  $k = 1, \dots, n$ .

*Proof.* Let  $k = 1, \dots, n$ . From the Pythagorean theorem, Fact 5, (18), and Theorem 6.ii we get

$$\begin{aligned} \text{dist}(e_k, \mathcal{A}) &= \|P_{\mathcal{A}}e_k - e_k\|^2 = \|e_k - c_n\|^2 - \|P_{\mathcal{A}}e_k - c_n\|^2 \\ &= \frac{n-1}{n} - (d+1)^2 \|f_k - c_n\|^2 = \frac{n-1}{n} - (d+1)^2 (d-1)m^2 = 1 - \frac{d^2}{n}. \quad \square \end{aligned}$$

Note that  $\mathcal{A} \subset \{p \in \mathbb{R}^n : \sum_{j=1}^n p_j = 1\}$ . Hence  $c_n \perp \mathcal{A}$  and so  $\langle p - c_n, q - c_n \rangle = \langle p, q \rangle - \frac{1}{n}$  for  $p, q \in \mathcal{A}$ . Let  $\iota$  be the inversion in  $\mathcal{A}$  through  $c_n$ , given by  $\iota(p) := 2c_n - p$  for  $p \in \mathcal{A}$ . Now we can characterise  $\mathcal{A}$  more precisely. The following fact is the result of direct computation.

*Fact 6.* Let  $p \in \mathcal{A}$ . The following conditions are equivalent:

- i.  $p \in \Delta$ ;
- ii.  $p_k \geq 0$  for every  $k = 1, \dots, n$ ;
- iii.  $\langle p, f_k \rangle \geq dm^2$  for every  $k = 1, \dots, n$ ;
- iv.  $\langle p, q \rangle \geq dm^2$  for every  $q \in D$ ;
- v.  $m^2 \geq \langle p - c_n, q - c_n \rangle$  for every  $q \in \iota(D)$ .

*Fact 7.*  $B_{\mathcal{A}}(c_n, r)$  is the inscribed (maximal central) ball contained in  $\Delta$ .

*Proof.* Taking  $\rho'_k := (I - \rho_k)/(d-1)$  and  $f'_k := p_{\Pi}(\rho'_k)$ , from the similarity of  $\mathcal{S}(\mathbb{C}^d)$  and  $\mathcal{Q}_{\Pi}$  we get  $\|f'_k - c_n\|^2 = dm^2 \|\rho'_k - I/d\|_{HS}^2 = \frac{m^2}{d-1} = r^2$  and  $\langle f'_k, f_k \rangle = dm^2(\text{tr}(\rho'_k \rho_k) + 1) = dm^2$ . Thus from Fact 6 it follows that  $f'_k \in \partial_{\mathcal{A}}\Delta \cap B(c_n, r)$ .  $\square$

Now we discuss the polarity of basic and primal polytopes.

**Definition 6.** Let  $C$  be a convex subset of  $\mathcal{A}$ ,  $s > 0$ . Define *polar* and *dual* of  $C$  in  $\mathcal{A}$  with respect to the central sphere (with centre at  $c_n$ ) of radius  $s$  by

$$C^{\circ} := \{p \in \mathcal{A} : s^2 \geq \langle p - c_n, q - c_n \rangle \text{ for every } q \in C\} \quad \text{and} \quad C^{\star} := \iota(C^{\circ})$$

Note that  $C^{\star} = \{p \in \mathcal{A} : \langle p, q \rangle \geq \frac{1}{n} - s^2 \text{ for every } q \in C\}$ .

From the convex analysis we know that

*Fact 8.* In the above situation

- i.  $C^{\circ\circ} = C$ ;
- ii.  $C^{\star} = (\iota(C))^{\circ}$ ;
- iii.  $C^{\star\star} = C$ .

Note that the last statement is a direct consequence of the preceding two. Two convex sets  $C$  and  $G$  are called *polar* (resp. *dual*) in  $\mathcal{A}$  with respect to the central sphere of radius  $s$  if  $C^{\circ} = G$  (resp.  $C^{\star} = G$ ). From condition (v) in Fact 6 we deduce

**Theorem 11.** *The polytopes  $D$  and  $\Delta$  are dual in  $\mathcal{A}$  with respect to the central sphere of radius  $m = \sqrt{rR}$ . The same is true for the balls  $B_{\mathcal{A}}(c_n, r)$  and  $B_{\mathcal{A}}(c_n, R)$ .*

Now, we show that the elements of  $\mathcal{Q}_{\Pi}$  fulfil the following *fundamental inequalities*

**Theorem 12.** *For  $p, q \in \mathcal{Q}_{\Pi}$  we have*

$$dm^2 \leq \langle p, q \rangle \leq 2dm^2.$$

*Proof.* Take  $\rho, \sigma \in \mathcal{S}(\mathbb{C}^d)$  such that  $p_{\Pi}(\rho) = p$  and  $p_{\Pi}(\sigma) = q$ . From the similarity of  $\mathcal{S}(\mathbb{C}^d)$  and  $\mathcal{Q}_{\Pi}$  it follows that  $\langle p, q \rangle = dm^2(\text{tr}(\rho\sigma) + 1)$ . Now, it is enough to apply the well-known inequality  $0 \leq \text{tr}(\rho\sigma) \leq 1$ .  $\square$

Finally, let us set  $s = m$  in the definition of dual sets. Then

**Theorem 13.** *The probability range  $\mathcal{Q}_{\Pi}$  is self-dual, i.e.*

$$\mathcal{Q}_{\Pi}^{\star} = \mathcal{Q}_{\Pi}.$$

*Proof.* It follows from the first inequality in Theorem 12 that  $\mathcal{Q}_{\Pi} \subset \mathcal{Q}_{\Pi}^{\star}$ . Let  $p \in \mathcal{Q}_{\Pi}^{\star}$  and  $\tau \in \mathcal{L}_s(\mathbb{C}^d)$  be such that  $\text{tr}\tau = 1$  and  $p = p_{\Pi}(\tau)$ . Since (2) holds for all  $\rho, \sigma \in \mathcal{L}_s(\mathbb{C}^d)$  such that  $\text{tr}\rho = \text{tr}\sigma = 1$ , from the definition of duality we get  $\text{tr}(\tau\rho) \geq 0$  for every  $\rho \in \mathcal{S}(\mathbb{C}^d)$ . Hence  $\tau \geq 0$  and, in consequence,  $\tau \in \mathcal{S}(\mathbb{C}^d)$  and  $p \in \mathcal{Q}_{\Pi}$ .  $\square$

## ACKNOWLEDGEMENTS

We thank Anna Szczepanek for remarks that improve the readability of the paper. AS is supported by Grant No. 2016/21/D/ST1/02414 of the Polish National Science Centre. WS is supported by Grant No. 2015/18/A/ST2/00274 of the Polish National Science Centre.

## REFERENCES

- [1] Amaral, B, Terra Cunha, M, On Graph Approaches to Contextuality and their Role in Quantum Theory, Springer, 2018.
- [2] Appleby, M, Fuchs, CA, Stacey, BC, Zhu, H, Introducing the Qplex: a novel arena for quantum theory, Eur. Phys. J. D 71 (2017), 197.
- [3] Appleby, DM, Ericsson, A, Fuchs, CA, Properties of QBist state spaces, Found. Phys. 41 (2011), 564–579.
- [4] Bang, S, Hiraki, A, Koolen, JH, Delsarte clique graphs, European J. Combin. 28 (2007), 501–516.
- [5] Belovs, A, Smotrovs, J, A criterion for attaining the Welch bounds with applications for mutually unbiased bases, in Calmet, J, Geiselmann, W, Müller-Quade, J (Eds), Mathematical Methods in Computer Science, MMICS 2008, Karlsruhe, Germany, December 17-19, 2008 - Essays in Memory of Thomas Beth, pp. 50-69.
- [6] Bengtsson, I, Życzkowski, K, Geometry of Quantum States. An Introduction to Quantum Entanglement, 2nd ed., Cambridge UP, 2017.
- [7] Bengtsson, I, Życzkowski, K, On discrete structures in finite Hilbert spaces, arXiv:1701.07902 [quant-ph].
- [8] Blokhuis, A, Brouwer, AE, Uniqueness of a Zara graph on 126 points and non-existence of a completely regular two-graph on 288 points, in de Doelder, PJ, de Graaf, J, van Lint, JH (Eds), Papers dedicated to J. J. Seidel. EUT Report 84-WSK-03. Eindhoven, Netherlands: Technische Hogeschool Eindhoven, 1984, pp. 6–19.
- [9] Bodmann, BG, Haas, JI, A short history of frames and quantum designs, arXiv:1709.01958 [quant-ph].
- [10] Brandsen, S, Dall’Arno, M, Szymusiak, A, Communication capacity of mixed quantum  $t$ -designs, Phys. Rev. A 94 (2016), 022335.
- [11] Brouwer, AE, Cohen, AM, Neumaier, A, Distance Regular Graphs, Springer, 1989.
- [12] Brouwer, AE, van Maldeghem, H, Strongly Regular Graphs, <https://homepages.cwi.nl/~aeb/math/srg/rk3/srgw24.pdf>
- [13] Brunner, N, Cavalcanti, D, Pironio, S, Scarani, V, Wehner, S, Bell nonlocality, Rev. Mod. Phys. 86 (2014), 419–478.
- [14] Bub, J, Bananaworld. Quantum Mechanics for Primates, Oxford UP, 2016.
- [15] Byrd, MS, Khaneja, N, Characterization of the positivity of the density matrix in terms of the coherence vector representation, Phys. Rev. A 68 (2003), 062322.
- [16] Cabello, A., Severini, S., Winter, A., (Non-)contextuality of physical theories as an axiom, arXiv:1010.2163 [quant-ph].
- [17] Cabello, A., Severini, S., Winter, A., Graph-theoretic approach to quantum correlations, Phys. Rev. Lett. 112 (2014), 040401.
- [18] Conway, JH, Wales, DB, Construction of the Rudvalis group of order 145, 926, 144, 000, J. Algebra 27 (1973), 538–548.
- [19] Coxeter, HSM, Regular complex polytopes, Cambridge UP, 1974.
- [20] Coxeter, HSM, Shephard, GC, Portraits of a family of complex polytopes, Leonardo 25 (1992), 239–244.
- [21] Crnković, D, Mikulić V, Rodrigues, BG, Some strongly regular graphs and self-orthogonal codes from the unitary group  $U_4(3)$ , Glas. Mat. Ser. III 45 (2010), 307–323.
- [22] Dall’Arno, M, Accessible information and informational power of quantum 2-designs, Phys. Rev. A 90 (2014), 052311.
- [23] Dall’Arno, M, D’Ariano, GM, Sacchi, MF, Informational power of quantum measurement, Phys. Rev. A 83 (2011), 062304.
- [24] DeBroda, JB, Fuchs, CA, Stacey, BC, Triply positive matrices and quantum measurements motivated by QBism, arXiv:1812.08762v2 [quant-ph].
- [25] DeBroda, JB, Fuchs, CA, Stacey, BC, Symmetric informationally complete measurements identify the essential difference between classical and quantum, Phys. Rev. Research 2 (2020), 013074.
- [26] DeBroda, JB, Fuchs, CA, Stacey, BC, Analysis and synthesis of minimal informationally complete quantum measurements, arXiv:1812.08762 [quant-ph].
- [27] Delsarte, P, Goethals, JM, Seidel, JJ, Bounds for systems of lines, and Jacobi polynomials, Philips Res. Repts. 30 (1975), 91-105.
- [28] Egan, M, Properties of tight frames that are regular schemes, Cryptogr. Commun. (2019), <https://doi.org/10.1007/s12095-019-00378-2>.
- [29] Fritz, T, Polyhedral duality in Bell scenarios with two binary observables, J. Math. Phys. 53 (2012), 072202.
- [30] Fuchs, CA, Schack, R, Quantum-Bayesian coherence, arXiv:0906.2187 [quant-ph].
- [31] Fuchs, CA, Schack, R, A Quantum-Bayesian route to quantum-state space, Found. Phys. 41 (2011), 345–356.
- [32] Fuchs, CA, Schack, R, Quantum-Bayesian coherence, Rev. Mod. Phys. 85 (2013), 1693–1715.
- [33] Fuchs, CA, Schack, R, Quantum-Bayesian coherence: The no-nonsense version, arXiv:1301.3274 [quant-ph].
- [34] Fuchs, CA, Hoang, MC, Stacey, BC, The SIC question: History and state of play, Axioms 6 (2017), 21.
- [35] Geller, J, Piani, M, Quantifying non-classical and beyond-quantum correlations in the unified operator formalism, J. Phys. A 47 (2014), 424030.
- [36] Goh, KT, Kaniewski, J, Wolfe, E, Vértesi, T, Wu, X, Cai, Y, Liang, Y-C, Scarani, V, Geometry of the set of quantum correlations, Phys. Rev. A 97 (2018), 022104.
- [37] Graydon, MA, Conical designs and categorical Jordan algebraic post-quantum theories, PhD Thesis, University of Waterloo, 2017.
- [38] Gross, D, Audenaert, K, Eisert, J, Evenly distributed unitaries: On the structure of unitary designs, J. Math. Phys. 48 (2007), 052104.
- [39] Grötschel, M., Lovász, L., Schrijver, A., Geometric algorithms and combinatorial optimization, 2nd ed., Springer, 1993.

- [40] Heinosaari, T, Jivulescu, MA, Nechita, I, Random positive operator valued measures, arXiv:1902.04751 [quant-ph].
- [41] Higman, DG, Finite permutation groups of rank 3, *Math. Z.* 86 (1964), 145–156.
- [42] Hirschfeld, JWP, On the history of generalized quadrangles, *Bull. Belg. Math. Soc. Simon Stevin* 3 (1994), 417–421.
- [43] Hoggar, SG,  $t$ -designs in projective spaces, *Europ. J. Combin.* 3 (1982), 233–254.
- [44] Hoggar, SG, A complex polytope as generalized quadrangle, *Proc. Roy. Soc. Edinburgh Sect. A* 95 (1983), 1–5.
- [45] Hoggar, SG, Parameters of  $t$ -designs in  $\mathbb{F}P^{d-1}$ , *European J. Combin.* 5 (1984), 29–36
- [46] Hughes, D, Waldron, S, Spherical  $(t, t)$ -designs with a small number of vectors, <https://www.math.auckland.ac.nz/~waldron/Preprints/Numerical-t-designs/numerical-t-designs.pdf>
- [47] Jones, NS, Linden, N, Parts of quantum states, *Phys. Rev. A* 71 (2005), 012324.
- [48] Kiktenko, EO, Malyshev, AO, Mastiukova, AS, Man'ko, VI, Fedorov, AK, Chruściński D., Probability representation of quantum dynamics using pseudo-stochastic maps, arXiv:1908.03404 [quant-ph].
- [49] Klappenecker, A, Rötteler, M, Mutually unbiased bases are complex projective 2-designs, in *Proc IEEE International Symposium on Information Theory, Adelaide, Australia, 4-9 September, IEEE, 2005*, pp. 1740–1744.
- [50] Knuth, D, The sandwich theorem. *Electron. J. Combin.* 1 (1994), A1.
- [51] Kwapisz, J, Trace optimality of SIC POVMs, *J. Phys. A: Math. Theor.* 52 (2019), 115203.
- [52] Levenshtein, VI, Designs as maximum codes in polynomial metric spaces, *Acta Appl. Math.*, 29 (1992), 1–82.
- [53] Lehrer GI, Taylor, DE, *Unitary Reflection Groups*, Cambridge UP, 2009.
- [54] Massad JE, Aravind, PK, The Penrose dodecahedron revisited, *Am. J. Phys.* 67 (1999), 631–638.
- [55] Mitchell, HH, Determination of all primitive collineation groups in more than four variables which contain homologies, *Amer. J. Math.* 36 (1914), 1–12.
- [56] Neumaier, A, *Combinatorial configurations in terms of distances*, Memorandum 81-09 (Dept. of Mathematics), Eindhoven University of Technology, 1981.
- [57] Neumaier, A, Regular cliques in graphs and special  $1\frac{1}{2}$  designs, in Cameron, PJ, Hirschfeld, JWP, Hughes, DR (Eds), *Finite Geometries and Designs, Proc. Second Isle of Thorns Conference*, Cambridge UP, 1981, pp. 244–259.
- [58] Oreshkov, O, Calsamiglia, J, Muñoz Tapia, R, Bagan, E, Optimal signal states for quantum detectors, *New J. Phys.* 13 (2011), 073032.
- [59] Payne, SE, All generalized quadrangles of order 3 are known, *J. Combin. Theory Ser. A* 18 (1975), 203–206.
- [60] Payne, SE, Thas, JA, *Finite generalized quadrangles*, 2nd ed., EMS, 2009.
- [61] Penrose, R, On Bell non-locality without probabilities: some curious geometry, preprint, Mathematical Institute, Oxford, 1992, published as Ellis J, Amati DD (Eds), *Quantum Relections (in honour of J.S. Bell)*, Cambridge UP, 2000, pp. 1–27.
- [62] Penrose, R, *Shadows of the Mind*, Oxford UP, 1994.
- [63] Pitowsky, I, The range of quantum probability, *J. Math. Phys.* 27 (1986), 1556–1565.
- [64] Polster, B, *A Geometrical Picture Book*, Springer, 1998.
- [65] Popescu, S, Rohrlich, D, Quantum nonlocality as an axiom, *Found. Phys.* 24 (1994), 379–385.
- [66] Popescu, S, Nonlocality beyond quantum mechanics, *Nature Physics* 10 (2014), 264–270.
- [67] Rosado, JI, Representation of quantum states as points in a probability simplex associated to a SIC-POVM, *Found. Phys.* 41 (2011), 1200–1213.
- [68] Saniga, M, On the Veldkamp space of  $GQ(4, 2)$ , *Int. J. Geom. Methods M.* 8 (2011), 39–47.
- [69] Scott, AJ, Tight informationally complete quantum measurements, *J. Phys. A: Math. Gen.* 39 (2006), 13507–13530.
- [70] Słomczyński, W, Szymusiak, A, Highly symmetric POVMs and their informational power, *Quantum Inf. Process.* 15 (2016), 565–606.
- [71] Soicher, LH, On cliques in edge-regular graphs, *J. Algebra* 421 (2015), 260–267.
- [72] Szymusiak, A, Maximally informative ensembles for SIC-POVMs in dimension 3, *J. Phys. A* 47 (2014), 445301.
- [73] Szymusiak, A, Pure states of maximum uncertainty with respect to a given POVM, *to appear in* *Open Syst. Inf. Dyn.*, arXiv:1701.01139v2 [quant-ph].
- [74] Szymusiak, A, Słomczyński, W, Informational power of the Hoggar symmetric informationally complete positive operator-valued measure, *Phys. Rev. A* 94 (2016), 012122.
- [75] Stacey, BC, Quantum theory as symmetry broken by vitality, arXiv:1907.02432v3 [quant-ph].
- [76] Tabia, GNM, Appleby, DM, Exploring the geometry of qutrit state space using symmetric informationally complete probabilities, *Phys. Rev. A* 88 (2013), 012131.
- [77] Talata, I, A volume formula for medial sections of simplices, *Discrete Comput. Geom.* 30 (2003), 343–353.
- [78] Waegell, M, Aravind, PK, The Penrose dodecahedron and the Witting polytope are identical in  $\mathbb{C}P^3$ , *Phys. Lett. A* 381 (2017), 1863–1857.
- [79] Waldron, S, *An introduction to finite tight frames*, Birkhäuser, 2018.
- [80] Weis, S, Quantum convex support, *Linear Alg. Appl.* 435 (2011), 3168–3188.
- [81] Welch, LR, Lower bounds on the maximum cross correlations of signals. *IEEE Transactions on Information Theory*, 20 (1974), 397–399.
- [82] Yetter, DN, On a formula relating volumes of medial sections of simplices, *Discrete Comput. Geom.* 43 (2010), 339–345.
- [83] Zimba, J, Penrose, R, On Bell non-locality without probabilities: more curious geometry, *Stud. Hist. Philos. Sci.* 24 (1993), 697–720.
- [84] Zhu, H, Multiqubit Clifford groups are unitary 3-designs, *Phys. Rev. A* 96 (2017), 062336.

INSTITUTE OF MATHEMATICS, JAGIELLONIAN UNIVERSITY, ŁOJASIEWICZA 6, 30-348 KRAKÓW, POLAND  
*E-mail address:* [anna.szymusiak@uj.edu.pl](mailto:anna.szymusiak@uj.edu.pl)  
*E-mail address:* [wojciech.slomczynski@im.uj.edu.pl](mailto:wojciech.slomczynski@im.uj.edu.pl)